The Quantitative Comparison of Grid Re-analysis Rainfall Products, Satellite Rainfall Products, and Hourly Rainfall Gauge Observation over Bali Province

by 088_063 -

The Quantitative Comparison of Grid Re-analysis Rainfall Products, Satellite Rainfall Products, and Hourly Rainfall Gauge Observation over Bali Province

Putu Aryastana[1, a)], Putu Ika Wahyuni[1, 2, b)], Listya Dewi[2, c)], Jason Pajimola Punay[3, d)], I Gusti Ngurah Hesa Respati Haditama[1, e)], Surya Pramod Jalakam[4, f)]

[1]*Department of Civil Engineering, Warmadewa University, Bali 80235, Indonesia*
[2]*Master Program of Infrastructure and Environmental Engineering, Warmadewa University, Bali 80235, Indonesia*
[3]*Department of Physics, College of Science, Bicol University, Legazpi City 4500, Philippines*
[4]*Department of Atmospheric Sciences, National Central University, Taoyuan 32001, Taiwan*

[a)] Corresponding author: aryastanaputu@yahoo.com
[b)]ikawahyuni9971@gmail.com
[c)]mynameisdewik516@gmail.com
[d)]jppunay@bicol-u.edu.ph
[e)]hesa.respatihaditama@warmadewa.ac.id
[f)]suryapramod24@gmail.com

Abstract. Grid re-analysis and satellite-based rainfall products provide rainfall data estimation on regional and global scales which have the potential to be used in many water resources management studies. Various rainfall product estimates are available for various features in the retrieval algorithm, sensor instrument used, spatial-temporal resolution, and coverage area. The objective of this study was to assess the performance of grid re-analysis rainfall product (ERA-5) and satellite rainfall product (IMERG) against hourly rain gauge observation over Bali Province from 2017 and 2020. The traditional comparison point-to-pixel-based method and quantitative statistical evaluation using continuous, categorical, and volumetric statistical indexes are implemented to evaluate satellite products. The comparative findings illustrate that IMERG exhibits superior performance at sub-daily scales in accurately detecting volume, whereas ERA-5 demonstrates greater capability in identifying rainfall events. Both products display a tendency to overestimate the capture of low to moderate rainfall events and to underestimate heavy to very heavy rainfall events. The IMERG product excels across various elevations. The significance of this study lies in its recognition of the dependability of re-analysis and satellite rainfall products. These products can serve as viable alternatives to rainfall station measurements in hydrology and water resources management research. Furthermore, this research extends its contribution to the governmental sector by promoting the utilization of satellite imagery technology and modeling as substitutes for rain gauge observations, especially in remote and mountainous areas.

INTRODUCTION

Rainfall, as a fundamental component of the water cycle, exerts profound effects on water storage, human endeavors, industries, agriculture, the ecosystem, economic development, and the intricate climate system [1]–[3]. Rainfall information can be procured through both direct and indirect measurement methodologies. Conventionally, rain gauge stations serve as the primary source of rainfall data, acquired through direct measurements at specific locations [4],[5]. The scarcity of rain gauge stations, coupled with their uneven dispersion, is most pronounced in remote and mountainous terrains, as well as oceanic regions. Overcoming this limitation is pivotal to achieving effective spatial coverage [4],[6],[7]. A complementary alternative lies in ground radar, capable of furnishing localized rainfall data over a continuous temporal spectrum and with comprehensive spatial coverage. The radar calculates rainfall intensity by translating reflectivity values [4]. However, the precision of radar-based rainfall estimates remains subject to atmospheric conditions, distance range, and elevation, particularly in mountainous landscapes [8],[9]. It's worth noting that both rain gauge stations and ground radar possess constraints pertaining to spatial coverage, especially in mountainous regions and over open waters [4].

Advancements in recent times have led to the emergence of gridded rainfall products (GRPs), which can be broadly categorized into three distinct groups delineated by variations in data sources and retrieval methodologies. These classifications encompass interpolated precipitation datasets generated from ground-based networks [10], precipitation datasets dependent on satellite technology obtained through visible/infrared/microwave precipitation estimations on a near-global scale [11], and reanalysis-derived precipitation datasets featuring predictive modeling and data assimilation processes. These processes establish connections between models and observations from diverse origins, including satellite and in-situ data sources [12]. Validation is typically essential prior to the utilization of GRPs in hydrological and meteorological contexts.

Diverse research endeavors have showcased the efficacy of gridded rainfall datasets across global and regional scales [13],[14], as well as temporal [15], seasonal [16], and climatological contexts [17]. These datasets have been assessed in intricate terrains [18],[19] and varying levels of rainfall intensities [20],[21]. Findings from earlier investigations have yielded disparate outcomes concerning the effectiveness of GRPs. To enhance their efficiency, endeavors are ongoing to incorporate diverse input data categories and refine estimation methodologies within algorithmic advancements, informed by these assessment outcomes. As a consequence, the appraisal of GRPs ' performance necessitates an ongoing alignment with algorithmic developments to ensure consistent enhancement.

Exploration into the performance evaluation of GRPs in the context of Bali remains exceedingly limited. GRP assessment within Bali's domain has been undertaken for a subset of products, including Tropical Rainfall Measuring Mission (TRMM), Climate Prediction Center Morphing Algorithm (CMOPRH), Precipitation Estimation from Remotely Sensed Information Using Artificial Neural Networks (PERSIANN), Integrated Merged MultisatellitE Retrievals for Global Precipitation Measurement/GPM (IMERG), Global Satellite Mapping of Precipitation (GSMaP), and Climate Hazards Group InfraRed Precipitation with Station (CHIRPS) [15],[17],[22]. To the best of our knowledge, there are no studies that have assessed the performance of the IMERG and European Centre for Medium-Range Weather Forecasts Reanalysis v5 (ERA-5) products over the island of Bali.

By and large, the precipitation patterns experienced in Bali are influenced by the climate system of the maritime continent, coupled with localized dynamics arising from interactions between land and sea. Moreover, the intricate terrain of Bali, characterized by complex features, substantially contributes to the fluctuations in rainfall. This terrain-related aspect holds the potential to exert a noteworthy impact on the performance of GRPs [23]. Consequently, it becomes imperative to comprehensively evaluate the efficacy of GRPs across varying elevations before their application in diverse domains such as water resources management, climatology, flood monitoring, and landslide forecasting. This study's primary goal was to undertake a performance assessment of two specific rainfall products: the grid re-analysis rainfall product (ERA-5) and the satellite rainfall product (IMERG). This assessment was conducted by comparing their outcomes against the data collected from hourly rain gauge observations spanning the period from 2017 to 2020 in Bali Province.

DATA & METHODS

Study Area

The study was conducted within the geographical boundaries of Bali Province, Indonesia, encompassing coordinates ranging from 8.06°S to 8.85°S in latitude and 114.43°E to 115.71°E in longitude. The total land area under investigation spanned 5636.66 km², as illustrated in Figure 1. Bali boasts a tropical climate, characterized by biannual shifts brought about by the alternating monsoon winds [24]. Notably, the island's topography exhibits diverse elevations relative to sea level, ranging from 0 to 2959 meters.

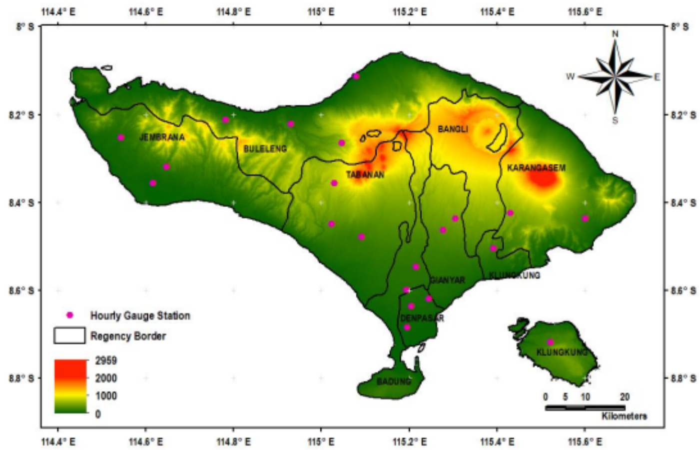

FIGURE 1. A map of Bali Province is provided, indicating the positions of rain gauge stations (depicted as purple dots), along with the names of the regencies and corresponding elevations.

Dataset

Hourly precipitation data spanning the timeframe from 2017 to 2020, sourced from Balai Wilayah Sungai Bali-Penida (BWSBP), have been employed for the purpose of this study. The selected GRPs encompass IMERG and ERA-5, spanning the period of 2017 to 2020. The current investigation utilized the latest Level-3 IMERG half-hourly dataset, retrieved from version-06B of the early run dataset. This dataset boasts a spatial resolution of 0.1°x0.1°, covering the latitude range of 60°N to 60°S, and temporal coverage spanning April 2014 to the present [25]. Notably, this dataset is accessible online at https://gpm.nasa.gov/data/directory, typically becoming available approximately four hours subsequent to the real-time data recording. The ERA-5 product employed in this research is characterized by a spatial resolution of 0.1° and a temporal resolution of an hour. It is accessible online and can be acquired for download through the link: https://cds.climate.copernicus.eu/cdsapp#!/dataset/10.24381/cds.e2161bac?tab=form.

Methods

To assess the compatibility of gauge rainfall data with the GRPs, a point-to-grid evaluation was undertaken, in line with methodologies outlined in previous studies [15],[26],[27]. The efficacy of the GRPs was evaluated across a spectrum of temporal scales, encompassing hourly, 3-hourly, 6-hourly, daytime, nighttime, and daily intervals. This evaluation was extended to include diverse elevations and varying rainfall intensities. The precision of the GRPs' hourly rainfall estimates was scrutinized in relation to the gradient of rainfall intensities. For the purpose of evaluation, hourly rainfall intensity was categorized into six distinct classes: < 0.1 mm (no rain), 0.1-1 mm (very low intensity), 1-5 mm (low intensity), 5-10 mm (moderate intensity), 10-20 mm (heavy intensity), and >20 mm (very heavy intensity). Furthermore, considering the distribution of rain gauge stations across different elevation levels, the performance of the GRPs was assessed with respect to terrain-induced effects. The elevation categorization employed for this assessment comprised two classes: > 1000 m (high elevation) and ≤1000 m (low elevation) [27].

The assessment of disparities between satellite estimations and actual observations encompassed a range of continuous statistical metrics, including mean error (ME), root mean square error (RMSE), bias ratio (BR), and correlation coefficient (R) [7],[18],[28], as frequently employed in previous studies. Furthermore, categorical statistics were employed to discern the capacity of satellite datasets in distinguishing occurrences of rainfall. This particular measurement was derived from a 2 × 2 contingency index, wherein 'hits' (H) indicated instances where both the rain gauge and satellite successfully identified rainfall events, 'false alarms' (F) represented situations where the satellite detected rainfall while the rain gauge did not, 'misses' (M) captured scenarios where the rain gauge identified rainfall but the satellite did not, and 'correct negatives' (CN) denoted instances where neither the satellite nor the rain gauge detected rainfall. From this index, three metrics emerged: probability of detection (POD), false alarm ratio (FAR), and critical success index (CSI) [28]. In addition, volumetric indices were developed, comprising the volumetric hit index

(VHI), volumetric false alarm ratio (VFAR), and volumetric critical success index (VCSI) [15],[27],[29],[30]. These indices were established to account for the volume of rainfall. Notably, a rainfall threshold (t) of 0.1 mm/hour was adopted to ascertain VHI, VFAR, and VCSI outcomes.

$$ME = \frac{1}{N}\sum_{i=1}^{N}(S_i - G_i) \tag{1}$$

$$RMSE = \sqrt{\frac{1}{N}\sum_{i=1}^{N}(S_i - G_i)^2} \tag{2}$$

$$BR = \frac{\sum S_i}{\sum G_i} \tag{3}$$

$$R = \frac{\sum_{i=1}^{N}(S_i - \bar{S})(G_i - \bar{G})}{\sqrt{\sum_{i=1}^{N}(S_i - \bar{S})^2}\sqrt{\sum_{i=1}^{N}(G_i - \bar{G})^2}} \tag{4}$$

$$POD = \frac{H}{H+M} \tag{5}$$

$$FAR = \frac{F}{H+F} \tag{6}$$

$$CSI = \frac{H}{H+M+F} \tag{7}$$

$$VHI = \frac{\sum_{i=1}^{N}\left(S_i \middle| (S_i > t \,\&\, G_i > t)\right)}{\sum_{i=1}^{N}\left(S_i \middle| (S_i > t \,\&\, G_i > t)\right) + \sum_{i=1}^{N}\left(G_i \middle| (S_i \leq t \,\&\, G_i > t)\right)} \tag{8}$$

$$VFAR = \frac{\sum_{i=1}^{N}\left(S_i \middle| (S_i > t \,\&\, G_i \leq t)\right)}{\sum_{i=1}^{N}\left(S_i \middle| (S_i > t \,\&\, G_i > t)\right) + \sum_{i=1}^{N}\left(S_i \middle| (S_i > t \,\&\, G_i \leq t)\right)} \tag{9}$$

$$VCSI = \frac{\sum_{i=1}^{N}\left(S_i \middle| (S_i > t \,\&\, G_i > t)\right)}{\sum_{i=1}^{N}\left(S_i \middle| (S_i > t \,\&\, G_i > t)\right) + \sum_{i=1}^{N}\left(G_i \middle| (S_i \leq t \,\&\, G_i > t)\right) + \sum_{i=1}^{N}\left(S_i \middle| (S_i > t \,\&\, G_i \leq t)\right)} \tag{10}$$

RESULT & DISCUSSION

The effectiveness of GRPs was evaluated across a spectrum of evaluation metrics. These encompassed continuous statistics (R, RMSE, BR, and ME), categorical measures (POD, FAR, and CSI), and volumetric indices (VHI, VFAR, and VCSI). The evaluation was conducted across various time scales (hourly, 3-hourly, 6-hourly, daytime, nighttime, and daily intervals), diverse levels of rainfall intensity, and varying elevations. Notably, the optimal performance of the GRPs was inferred from high values of R, POD, CSI, VHI, and VCSI, coupled with minimal values of ME, RMSE, FAR, VFAR, and BR. Values close to 1 for the latter set of metrics indicated a strong capability of the GRPs in estimation.

Performance Assessment on Various Time-Scales

The agreement between the GRPs and the gauge observations is assessed using the correlation coefficient (R), as illustrated in Figure 2a. Both GRPs exhibit a limited level of concordance with the rain gauge stations at hourly, 3-hourly, and 6-hourly intervals but demonstrate a moderate level of agreement on a daily scale. In general, IMERG exhibits significantly superior performance, boasting higher correlation coefficients across nearly all time scales when compared to ERA-5. Recent research validates that the latest iteration of IMERG has succeeded in enhancing its consistency with gauge measurements, resulting in increased R scores. In alignment with these contemporary findings, IMERG version 6 surpasses IMERG version 5 in representing the spatial characteristics of warm climate rainfall in Taiwan across various temporal scales [31]. This improvement may be attributed to the upgraded morphing algorithm from version 5 to version 6 [31]. Furthermore, IMERG outperforms ERA-5 products based on the Root Mean Square Error (RMSE) value, as depicted in Figure 2b. Both IMERG and ERA-5 products consistently underestimate rainfall when compared to rain gauge data, resulting in a Bias Ratio (BR) of less than one and negative Mean Error (ME) values. In the recent study, IMERG's superiority over ERA-5 products is affirmed through assessments involving R, RMSE, and ME values.

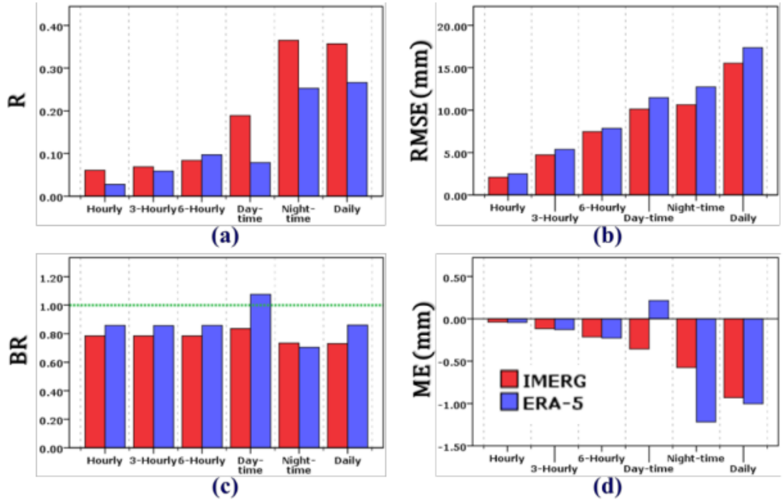

FIGURE 2. The ongoing statistical measurements across various temporal intervals encompass: (a) R, (b) RMSE, (c) BR, and (d) ME

Contingency analysis typically employs the Probability of Detection (POD), False Alarm Rate (FAR), and Critical Success Index (CSI) to quantitatively assess the performance of GRPs. As depicted in Figures 3a, 3b, and 3c, overall contingency scores are presented for the detection of rainy events using a 0.1 mm/hour threshold to distinguish between rainy and non-rainy occurrences. Figures 3a, 3b and 3c reveal that ERA-5 exhibits superior performance in terms of POD (ranging from 0.22 to 0.68) and CSI (ranging from 0.10 to 0.48), while IMERG outperforms ERA-5 in terms of FAR (ranging from 0.36 to 0.78). This performance distinction holds across various time scales, including hourly, 3-hourly, 6-hourly, daytime, nighttime, and daily scales. Notably, the ability of GRPs to detect rainfall events increases as the time scale increases. Statistical analysis supports the conclusion that satellite-derived products exhibit sufficient accuracy when compared to ground-based data in terms of accumulation [28]. Most categorical statistical analyses suggest that ERA-5 demonstrates a more favorable performance in detecting rainfall events compared to IMERG products.

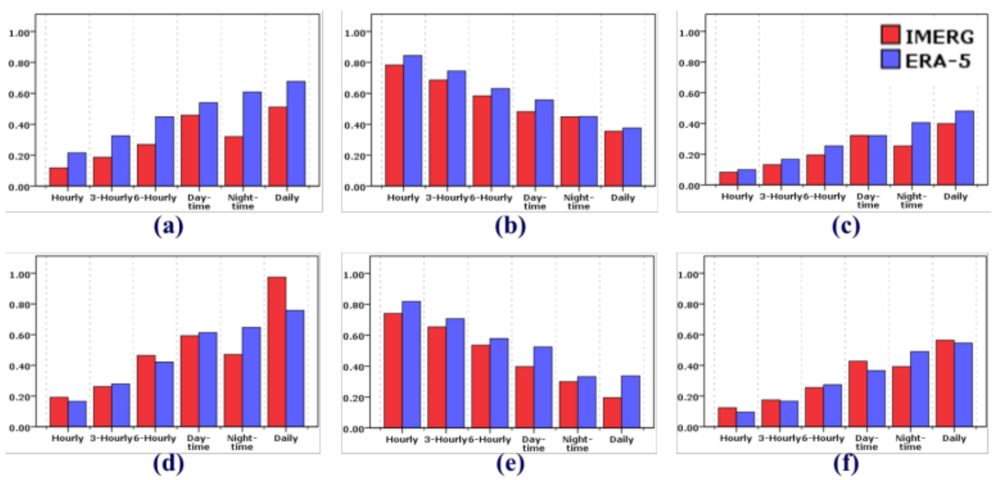

FIGURE 3. The categorical performance metrics and volumetric indicators across various temporal intervals consist of: (a) POD, (b) FAR, (c) CSI, (d) VHI, (e) VFAR, and (f) VCSI

Figures 3d, 3e, and 3f present the VHI, VFAR, and VCSI scores, respectively, for both the IMERG and ERA-5 products. The figures illustrate that both products exhibit their highest VHI and VCSI scores at the daily scale, but their lowest scores at the hourly scale. The IMERG product outperforms ERA-5 in terms of VHI, VFAR, and VCSI values across hourly, 3-hourly, 6-hourly, and daily scales. The IMERG product achieves VHI, VFAR, and VCSI scores ranging from 0.19 to 0.97, 0.2 to 0.74, and 0.12 to 0.56, respectively. This superiority can likely be attributed to IMERG's high temporal resolution, which enables it to more effectively capture regional variations in sub-daily precipitation frequency [15].

Performance Assessment on Rainfall Intensity

The probability distribution function (PDF), which provides valuable insights into the frequency distribution of a dataset, has been utilized in numerous research studies to assess the performance of GRPs [32]. In our current investigation, we employed the PDF to evaluate the performance of IMERG and ERA-5 in capturing the frequency of rainfall events at varying intensities. Figure 4 illustrates the PDF for our study area, where we calculated the PDF for hourly rainfall events spanning from January 2017 to December 2020. When compared to rain gauge data, all GRPs exhibited a tendency to underestimate the occurrence of heavy rainfall events (10-20 mm/hour) and very heavy rainfall events (>20 mm/hour), while overestimating the frequency of light rainfall events (1-5 mm/hour) and moderate rainfall events (5-10 mm/hour) (see Figure 4b and 4c). The overestimation of IMERG in detecting light and moderate rainfall may be attributed to the inclusion of two more advanced instruments, namely the Dual-frequency Precipitation Radar (DPR) and GPM Microwave Imager (GMI), designed to provide more precise instantaneous precipitation estimates, particularly for light rainfall [33]. Additionally, Figure 4a depicts IMERG tended to overestimate the frequency of non-rain events (>0.1 mm/hour), while ERA-5 tended to underestimate them. Furthermore, ERA-5 products tended to overestimate the frequency of very light rainfall events (0.1-1 mm/hour), whereas IMERG tended to underestimate them. The underestimation of GRPs in heavy to extreme rainfall might be attributed to the interpolation process used for classifying heavy rainfall [34]. Moreover, the presence of uncertainties in rainfall estimation techniques due to orographic influences and dense vegetation in specific locations can also contribute to the underestimation of GRPs in detecting heavy to extreme rainfall [35].

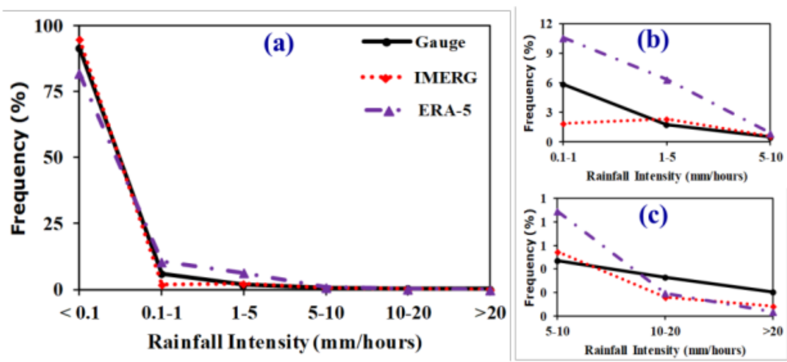

FIGURE 4. The probability distribution functions (PDFs) for rainfall occurrences as observed by rain gauges are as follows: (a) for all levels of rainfall intensities, (b) for low to moderate intensities, and (c) for moderate to very heavy intensities

Performance Assessment on Elevation

The terrain's impact may play a crucial role in shaping the effectiveness of GRPs [23]. The assessment across different elevations emphasizes the importance of using sub-daily rainfall data as a primary input for early warning systems in natural disaster mitigation [29]. Rainfall variability in the island region results from orographic uplift and varying terrain characteristics [36]. Terrain and altitude significantly influence rainfall patterns [37]. This study categorized the selected rain gauge stations into two groups based on their altitude: those at low altitudes (below 1000 meters) and those at high altitudes (above 1000 meters). Figure 5 presents a performance chart that offers a preview of the statistics demonstrating the accuracy of the three SPDs in detecting heavy rainfall events caused by typhoons in terms of BR, CSI, FAR, and POD. This graph effectively showcases the capabilities of the GRPs. This capability chart was initially introduced by Roebber to visually depict the relationship between various aspects of model performance [38]. The *x*-axis represents the success ratio or 1-FAR, while the *y*-axis represents the POD score. Dotted lines originating from the origin depict the BR score, with the no-bias scenario shown by the diagonal dotted line. The dashed contour lines represent the CSI score. The highest performance is observed in the upper right corner of the graph and along the diagonal dotted line. The performance graph demonstrates that both sets of GRPs exhibit moderate capabilities in accurately capturing rainfall across different elevations. Generally, the IMERG dataset performs well at various elevations. It tends to overestimate rainfall at most elevations, while ERA-5 underestimates rainfall at lower elevations. Conversely, ERA-5 tends to overestimate rainfall at higher elevations.

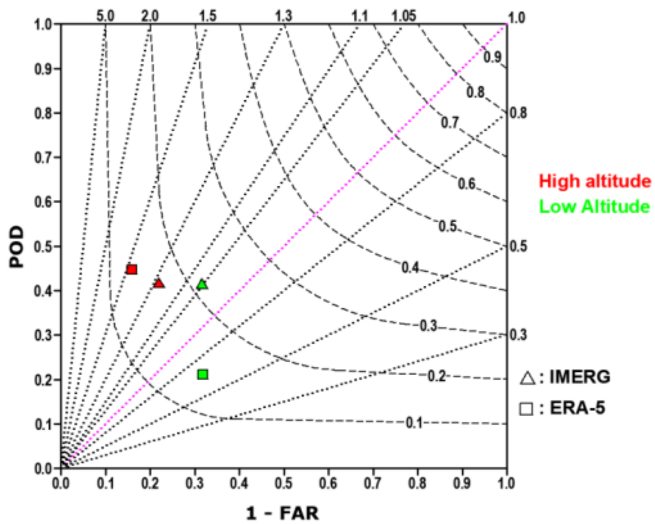

FIGURE 5. The performance diagram illustrates the GRPs at various altitudes. Distinct colors correspond to distinct altitudes (green for low altitude and red for high altitude)

CONCLUSION

To assess their performance quality, the present study conducted a comparison between the IMERG and ERA-5 products and rainfall gauge measurements on Bali Island during the period from 2017 to 2020. This comparison was conducted across different time scales (hourly, 3-hourly, 6-hourly, daytime, nighttime, and daily), considering terrain characteristics and varying rainfall intensities. The results of this comparative analysis reveal that IMERG demonstrates superior performance when it comes to accurately estimating rainfall volume at sub-daily time scales. On the other hand, ERA-5 exhibits greater proficiency in identifying rainfall events. It's noteworthy that both products tend to overestimate the capture of light to moderate rainfall events while underestimating heavy to extremely heavy rainfall events. Additionally, IMERG performs exceptionally well across diverse elevations. Obtaining precise rainfall data through satellite-based estimates remains a daunting task, particularly in regions characterized by intricate topography, severe weather occurrences, and high susceptibility to natural disasters. To delve deeper into this subject, it is advisable to assess the performance of GRPs over an extended duration under varying environmental conditions, such as different land cover types, slopes, evapotranspiration rates, and soil moisture levels.

ACKNOWLEDGMENTS

We express our gratitude to the data contributors for IMERG and ERA-5. Additionally, we extend our acknowledgments to the Balai Wilayah Sungai Bali-Penida under the Ministry of Public Works and Human Settlements of Indonesia for their invaluable assistance in procuring hourly gauge station rainfall data for the Bali province. This research received support from Warmadewa University, Bicol University, and National Central University.

REFERENCES

1. R. Gao, F. Li, X. Wang, T. Liu, D. Du, and Y. Bai, Atmos. Res. **193**, 204 (2017).
2. M. Kotz, A. Levermann, and L. Wenz, Nature **601**, 223 (2022).
3. L. Trinh-Tuan, J. Matsumoto, T. Ngo-Duc, M.I. Nodzu, and T. Inoue, Prog. Earth Planet. Sci. **6**, (2019).
4. H. Feidas, Theor. Appl. Climatol. **99**, 193 (2010).
5. P. Salio, M.P. Hobouchian, Y. García Skabar, and D. Vila, Atmos. Res. **163**, 146 (2015).
6. X. Ji, Y. Li, X. Luo, D. He, R. Guo, J. Wang, Y. Bai, C. Yue, and C. Liu, Atmos. Res. **242**, 104964 (2020).
7. E.I. Nikolopoulos, E. Destro, V. Maggioni, F. Marra, and M. Borga, J. Hydrometeorol. **18**, 2207 (2017).
8. Z. Li, D. Yang, and Y. Hong, J. Hydrol. **500**, 157 (2013).
9. J. Zhang, K. Howard, C. Langston, S. Vasiloff, B. Kaney, A. Arthur, S. Van Cooten, K. Kelleher, D. Kitzmiller, F. Ding, D.-J. Seo, E. Wells, and C. Dempsey, Bull. Am. Meteorol. Soc. **92**, 1321 (2011).
10. A. Yatagai, K. Kamiguchi, O. Arakawa, A. Hamada, N. Yasutomi, and A. Kitoh, Bull. Am. Meteorol. Soc. **93**, 1401 (2012).
11. H. Ashouri, K.-L. Hsu, S. Sorooshian, D.K. Braithwaite, K.R. Knapp, L.D. Cecil, B.R. Nelson, and O.P. Prat, Bull. Am. Meteorol. Soc. **96**, 69 (2015).
12. L. Bengtsson, J. Geophys. Res. **109**, D11111 (2004).
13. W.F. Krajewski, G.J. Ciach, J.R. McCollum, and C. Bacotiu, J. Appl. Meteorol. **39**, 1071 (2000).
14. Q. Jiang, W. Li, Z. Fan, X. He, W. Sun, S. Chen, J. Wen, J. Gao, and J. Wang, J. Hydrol. **595**, 125660 (2021).
15. C.-Y. Liu, P. Aryastana, G.-R. Liu, and W.-R. Huang, Atmos. Res. **244**, 105032 (2020).
16. V. Thiemig, R. Rojas, M. Zambrano-Bigiarini, V. Levizzani, and A. De Roo, J. Hydrometeorol. **13**, 1760 (2012).
17. N. Rahmawati and M.W. Lubczynski, Theor. Appl. Climatol. **134**, 513 (2018).
18. R. Xu, F. Tian, L. Yang, H. Hu, H. Lu, and A. Hou, J. Geophys. Res. **122**, 910 (2017).
19. T.G. Romilly and M. Gebremichael, Hydrol. Earth Syst. Sci. **15**, 1505 (2011).
20. Y.C. Gao and M.F. Liu, Hydrol. Earth Syst. Sci. **17**, 837 (2013).
21. Y. Mei, E.N. Anagnostou, E.I. Nikolopoulos, and M. Borga, J. Hydrometeorol. **15**, 1778 (2014).
22. A.R. As-Syakur, T. Tanaka, R. Prasetia, I.K. Swardika, and I.W. Kasa, Int. J. Remote Sens. **32**, 8969 (2011).
23. T. Dinku, F. Ruiz, S.J. Connor, and P. Ceccato, J. Appl. Meteorol. Climatol. **49**, 1004 (2010).
24. E. Aldrian, L.D. Gates, and F.H. Widodo, MPI Rep. (2003).
25. G.J. Huffman, D.T. Bolvin, D. Braithwaite, K.-L. Hsu, R. Joyce, C. Kidd, E.J. Nelkin, S. Sorooshian, J. Tan, and P. Xie, Natl. Aeronaut. Sp. Adm. 1 (2019).
26. A.A. Fenta, H. Yasuda, K. Shimizu, Y. Ibaraki, N. Haregeweyn, T. Kawai, A.S. Belay, D. Sultan, and K. Ebabu, Atmos. Res. **212**, 43 (2018).
27. P. Aryastana, C.-Y. Liu, B. Jong-Dao Jou, E. Cayanan, J.P. Punay, and Y. Chen, Earth Sp. Sci. **9**, (2022).
28. E.E. Ebert, in *Meas. Precip. from Sp. EURAINSAT Futur.* (Springer, 2007), pp. 345–356.
29. G.T. Ayehu, T. Tadesse, B. Gessesse, and T. Dinku, Atmos. Meas. Tech. **11**, 1921 (2018).
30. A. Aghakouchak and A. Mehran, Water Resour. Res. **49**, 7144 (2013).
31. W.-R. Huang, P.-Y. Liu, Y.-H. Chang, and C.-Y. Liu, Remote Sens. **12**, 347 (2020).
32. Y. Ma, Y. Yang, Z. Han, G. Tang, L. Maguire, Z. Chu, and Y. Hong, J. Hydrol. **556**, 634 (2018).
33. H. Chen, B. Yong, Y. Shen, J. Liu, Y. Hong, and J. Zhang, J. Hydrol. **581**, 124376 (2020).
34. J. Fang, W. Yang, Y. Luan, J. Du, A. Lin, and L. Zhao, Atmos. Res. **223**, 24 (2019).
35. M.T. Brunetti, M. Melillo, S. Peruccacci, L. Ciabatta, and L. Brocca, Remote Sens. Environ. **210**, 65 (2018).
36. K.-O. Lee, H. Uyeda, and D.-I. Lee, Atmos. Res. **135–136**, 76 (2014).
37. C. Chen, Z. Li, Y. Song, Z. Duan, K. Mo, Z. Wang, and Q. Chen, J. Hydrometeorol. **21**, 533 (2020).
38. P.J. Roebber, Weather Forecast. **24**, 601 (2009).

The Quantitative Comparison of Grid Re-analysis Rainfall Products, Satellite Rainfall Products, and Hourly Rainfall Gauge Observation over Bali Province

ORIGINALITY REPORT

26%	13%	23%	15%
SIMILARITY INDEX	INTERNET SOURCES	PUBLICATIONS	STUDENT PAPERS

PRIMARY SOURCES

1	Submitted to Universitas Warmadewa Student Paper	7%
2	Chian-Yi Liu, Putu Aryastana, Gin-Rong Liu, Wan-Ru Huang. "Assessment of satellite precipitation product estimates over Bali Island", Atmospheric Research, 2020 Publication	5%
3	Putu Aryastana, Chian-Yi Liu, Ben Jong-Dao Jou, Esperanza Cayanan, Jason Pajimola Punay, Ying-Nong Chen. "Assessment of Satellite Precipitation Data Sets for High Variability and Rapid Evolution of Typhoon Precipitation Events in the Philippines", Earth and Space Science, 2022 Publication	2%
4	assets.researchsquare.com Internet Source	2%
5	Ehsan Sharifi, Reinhold Steinacker, Bahram Saghafian. "Multi time-scale evaluation of	1%

high-resolution satellite-based precipitation products over northeast of Austria", Atmospheric Research, 2018
Publication

6	Submitted to University of Reading Student Paper	1 %
7	ojs.unik-kediri.ac.id Internet Source	1 %
8	www.researchgate.net Internet Source	1 %
9	Desalew Meseret Moges, Alexander Kmoch, Evelyn Uuemaa. "Application of satellite and reanalysis precipitation products for hydrological modeling in the data-scarce Porijõgi catchment, Estonia", Journal of Hydrology: Regional Studies, 2022 Publication	1 %
10	digitalcommons.unl.edu Internet Source	1 %
11	jmr.cmsjournal.net Internet Source	1 %
12	Chian-Yi Liu, Jason Pajimola Punay, Chun-Chieh Wu, Kao-Shen Chung, Putu Aryastana. "Characteristics of deep convective clouds, precipitation, and cloud properties of rapidly intensifying tropical cyclones in the western	<1 %

North Pacific", Journal of Geophysical Research: Atmospheres, 2022
Publication

13 Submitted to Imperial College of Science, Technology and Medicine — <1%
Student Paper

14 journals.ametsoc.org — <1%
Internet Source

15 K Hedberg Nyqvist. "Early oral behaviour in preterm infants during breastfeeding: an electromyographic study", Acta Paediatrica, 01/02/2007 — <1%
Publication

16 M. Laverde-Barajas, G.A. Corzo Perez, J.G. Dalfré Filho, D.P Solomatine. "Assessing the performance of near real-time rainfall products to represent spatiotemporal characteristics of extreme events: case study of a subtropical catchment in south-eastern Brazil", International Journal of Remote Sensing, 2018 — <1%
Publication

17 essd.copernicus.org — <1%
Internet Source

18 www.science.gov — <1%
Internet Source

19	Putu Aryastana, Chian-Yi Liu, Ben Jong-Dao Jou, Esperanza Cayanan, Jason Pajimola Punay, Ying-Nong Chen. "Assessment of satellite precipitation datasets for high variability and rapid evolution of typhoon precipitation events in the Philippines", Earth and Space Science, 2022 Publication	<1 %
20	acp.copernicus.org Internet Source	<1 %
21	ijesi.org Internet Source	<1 %
22	Kirubel Mekonnen, Naga Manohar Velpuri, Mansoor Leh, Komlavi Akpoti et al. "Accuracy of satellite and reanalysis rainfall estimates over Africa: A multi-scale assessment of eight products for continental applications", Journal of Hydrology: Regional Studies, 2023 Publication	<1 %
23	Rajani K. Pradhan, Yannis Markonis, Mijael Rodrigo Vargas Godoy, Anahí Villalba-Pradas et al. "Review of GPM IMERG performance: A global perspective", Remote Sensing of Environment, 2022 Publication	<1 %
24	downloads.hindawi.com Internet Source	<1 %

25 www.hindawi.com
Internet Source
<1 %

26 www.scilit.net
Internet Source
<1 %

27 Ashish Navale, Charu Singh, Sachin Budakoti, Sanjeev Kumar Singh. "Evaluation of season long rainfall simulated by WRF over the NWH region: KF vs. MSKF", Atmospheric Research, 2020
Publication
<1 %

28 Ruida Zhong, Xiaohong Chen, Chengguang Lai, Zhaoli Wang, Yanqing Lian, Haijun Yu, Xiaoqing Wu. "Drought monitoring utility of satellite-based precipitation products across mainland China", Journal of Hydrology, 2018
Publication
<1 %

29 Ruochen Sun, Huiling Yuan, Yize Yang. "Using multiple satellite-gauge merged precipitation products ensemble for hydrologic uncertainty analysis over the Huaihe River basin", Journal of Hydrology, 2018
Publication
<1 %

30 Wan-Ru Huang, Pin-Yi Liu, Jie Hsu. "Multiple timescale assessment of wet season precipitation estimation over Taiwan using the PERSIANN family products", International
<1 %

Journal of Applied Earth Observation and Geoinformation, 2021
Publication

31	worldwidescience.org Internet Source	<1 %
32	www.tandfonline.com Internet Source	<1 %

Exclude quotes	On	Exclude matches	Off
Exclude bibliography	On		